

Dynamics of Polystyrene Subchains of a Styrene–Methyl Methacrylate Diblock Copolymer in Solution Measured by Dynamic Light Scattering with an Isorefractive Index Solvent. 2. Semidilute Solution Region

Yoshisuke Tsunashima* and Yukinao Kawamata

Institute for Chemical Research, Kyoto University, Uji, Kyoto 611, Japan

Received October 19, 1993; Revised Manuscript Received January 5, 1994*

ABSTRACT: The dynamics of polystyrene (PS)-*block*-poly(methyl methacrylate) (PMMA) in the semidilute solution region was studied by dynamic light scattering measurements made on the benzene solutions of polymer mass concentration $c = 0.844c^* - 2.00c^*$ at 30 °C. The dynamic structure factor observed for the visible PS parts was expressed at all c and in $0.13 < qR_G < 1.54$ by the sum of two or three exponentials whose decay rates Γ_i were separated distinctly from each other. For the slow mode of the smallest Γ values, Γ was proportional to q^2 and the motion was assigned to the center-of-mass (or the long-time) diffusion motion of a single block chain in a pregel state, but the diffusion coefficient showed a change in its c dependence from c^{-1} to $c^{-1.76}$ with increasing c . For the medium mode, Γ was also proportional to q^2 and the diffusion coefficient value was about 4 times larger than that of the slow mode. This feature allowed us to assign this motion to be a cooperative diffusion of the PS concentration blob (the size ξ_H), but the c dependence of $D_{\text{coop,PS}} \propto c^{-1}$ at higher c was found to disagree with the scaling prediction in a good solvent, $D_{\text{coop}} \propto c^{0.75}$. The fast mode of the largest Γ values was independent of c but the Γ values showed a q^2 dependence at $(qR_G)^2 < 1.2$ and a q^{4-5} dependence at $(qR_G)^2 > 1.3$. These behaviors indicated that the former represents the relative motion of PS parts with respect to PMMA parts and the latter the Rouse dynamics, and totally the interdiffusion motion. In addition, there were some indications of the coupling between the cooperative diffusion and interdiffusions. The first cumulant Γ_0 , which shows the short-time behavior of the chain, was found to exhibit a clear transition from a rough q^2 dependence to a q^4 dependence at $q\xi_H \approx 0.6$. This means that even in a good solvent the internal motion of the diblock chain in the semidilute region can be represented by Rouse dynamics at $q\xi_H \geq 0.6$.

Introduction

The dynamics of a solution consisting of an A–B diblock copolymer in a solvent has features different from that of a ternary mixture composed of two homopolymers and a solvent and has recently been paid special attention. The reason is that in the A–B diblock copolymer solution the relative motion of subchains A and B involves the internal motions of the entire copolymer chains, the difference in the relaxation times of the internal and external motions of the chain being in need of a clear understanding of a concept on the short-time and long-time behavior of the chain. The dynamic light scattering (DLS) method of experiments can be suited in general for investigating such chain dynamics. Frequently in this case, the solvent has been chosen to be isorefractive with one of the subchains. The dynamics is then driven by the “visible” subchain part, which makes the interpretation easier.

Polystyrene (PS)-*block*-poly(methyl methacrylate) (PMMA) in benzene, part 1 in this series,¹ is an example of a few such systems studied for dilute solutions of A–B diblock copolymers. Benzene was used as a good solvent for both PS and PMMA subchains and was isorefractive with PMMA. Two dynamical modes of motion have been observed in this system and these two modes have been discussed in detail in view of the above-mentioned special concept indispensable for diblock copolymer chains of nature. For semidilute solutions of A–B diblock copolymers, on the other hand, PS-*block*-PMMA in toluene,^{2,3} PS-*block*-polyisoprene (PIP) in 1,1-diphenylethylene,⁴ and PS-*block*-PIP in toluene⁵ have been experimentally studied with the polymer mass concentrations $5c^*$, $1.6c^*$,³ $(1.1-7.5)c^*$,⁴ and $(2.5-3)c^*$,⁵ with c^* the overlapping polymer

concentration. The solvents used were good for both subchain parts and were isorefractive with a part of the subchain.²⁻⁴ These experiments have shown that there are two modes of motion in semidilute diblock copolymer solutions. The observed intermediate scattering function, i.e., the dynamic structure factor $S(q,t)$ at time t and the magnitude of the scattering vector q ($=|q|$), has been found to be represented by a superposition of two exponentials:

$$S(q,t) = A \exp(-\Gamma t) + A' \exp(-\Gamma' t) \quad (1)$$

The observed two modes have been suggested to be identified as the cooperative diffusion (a slow motion) and interdiffusion (a fast motion) processes of the pseudonet-work formed by the diblock chains in solution, and the observed relaxation frequencies Γ and Γ' have been related to the diffusion coefficients characterizing these processes, although some confusion has been detected in the magnitudes of these two modes.²⁻⁴ In the interpretation of these modes, the authors in refs 2–5 have referred to the normal modes of motion which have appeared in a theory of the dynamics of diblock copolymers in a solvent,⁶ as described below. This theory was derived first by Benmouna et al.,⁶ where they have been extending to a block copolymer solution system the theory of a solution of two homopolymer mixtures⁷ by using both the linear response theory to calculate the mobilities without including hydrodynamic interactions and the random phase approximation (RPA) to calculate the static structure factor $S(q)$. Allowing the two subchain parts A and B in A–B diblock copolymers to be the two polymer components in the system, Benmouna et al.⁶ have shown that $S(q,t)$ in any ternary mixture consisting of two polymers and a

* Abstract published in *Advance ACS Abstracts*, March 1, 1994.

Table 1. Static Characteristics of the PS-PMMA Diblock Copolymer, BMM313, in Benzene at 30.0 °C and the Solvent, Benzene, at 30 °C and at 488 nm^a

polymer code	styrene content, wt %	$10^{-6}M_w$	$10^4 A_2$, mol cm ³ g ⁻²	$10^{12} A_3$, mol cm ⁶ g ⁻³	R_G , nm
BMM313	38.5	1.53	1.67	-1.12	41.0
dn/dc , cm ³ g ⁻¹					
solvent	n_0	PS	PMMA	BMM313	
benzene	1.5060	0.1105	0.0003	0.0427	

^a Part 1 in this series.

solvent is expressed as a sum of two exponential normal modes (bimodal relaxation),

$$S(q, t) = A_1(q) \exp[-\lambda_1(q)t] + A_2(q) \exp[-\lambda_2(q)t] \quad (2)$$

with λ_i and A_i the relaxation frequency (the relaxation decay rate) and the fractional amplitude of the normal mode i , respectively; the expression of eq 2 is exactly the same as the earlier one for binary polymer solutions which has been derived from the general theory of multicomponent systems by Akcasu et al.⁸ Experimental results in refs 2–5 have thus indicated the validity of this simple two-mode theory and suggested the identification of the theoretical normal modes with the experimentally observed two modes of motion in the semidilute diblock copolymer solutions.

Very recently, however, Akcasu et al.^{9,10} have theoretically shown that $S(q, t)$ in an A-B diblock copolymer solution can be represented by two normal modes only in the short-time ($t \rightarrow 0$) and Markoff limits, as described already, but that the two modes cannot be identified in general as the cooperative diffusion and interdiffusion processes; the normal modes are independent of each other, but the cooperative diffusion and interdiffusion modes are in general coupled statistically, and the former and the latter modes can be identified with each other only when A and B subchains are identical and be distinguished from each other only by the labeling. Here the Markoff limit can be met by letting $q \rightarrow 0$ and $t \rightarrow \infty$ but keeping $q^2 t$ fixed.

In this work, we investigate through DLS the details of these dynamical modes of motion in the semidilute solution of diblock copolymers by using a system of a PS-PMMA diblock copolymer in benzene, a good solvent for both PS and PMMA that is isorefractive with PMMA. We intend to make clear the short-time and long-time behavior of the diblock chain and to discuss the questions about the number of dynamical modes existing in semidilute solutions of the diblock copolymer, the concentration and q dependences of these modes, and the identification of these modes as the theoretical normal modes or as the cooperative diffusion and interdiffusion processes.

Experimental Section

Polymer Sample, Characterization, and Solvent. A polystyrene (PS)-poly(methyl methacrylate) (PMMA) diblock copolymer was anionically prepared as described in part 1 of this series.¹ The sample, coded as BMM313, was characterized previously¹ by static light scattering and GPC, as listed in Table 1. The table shows that the sample has a narrow molecular weight distribution. Benzene, a solvent used, was of spectrograde one and its purity was ascertained by checking the refractive index n_0 at 30.0 °C in a Pulfrich refractometer (Shimadzu): $n_0 = 1.5060$ at 488 nm and 30 °C, and the viscosity $\eta_s = 5.621 \times 10^{-3}$ g cm⁻¹ s⁻¹ at 30 °C. As mentioned previously,¹ benzene is a good solvent with both PS and PMMA and is isorefractive with PMMA at 30.0 °C for a 488-nm line of an argon-ion laser (Table 1).

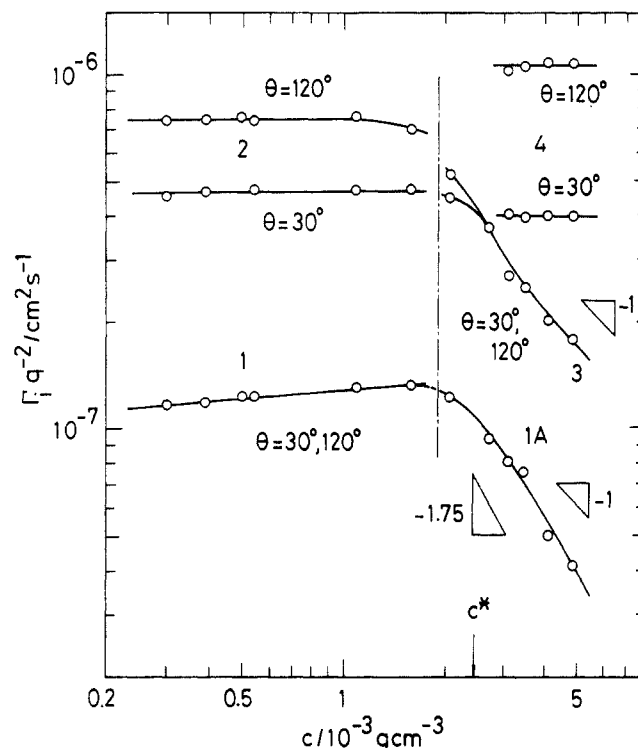


Figure 1. Typical q and c dependences of the mean decay rate $\Gamma_i(q, c)$ for the two or three modes of motion, $i = 1A, 3$, and 4 , for semidilute solutions of the PS-PMMA diblock copolymer in benzene at 30 °C shown to the right-hand side of a vertical chain line. The Γ_i/q^2 behavior at $qR_G \ll 1$ and $qR_G > 1$ is represented by the curves at the scattering angles $\theta = 30$ and 120° , respectively. The left-hand side of the vertical chain line indicates the dilute solution region (previous work), where modes 1 and 2 have been detected.

Therefore, PMMA subchains of the diblock copolymer BMM313 are masked optically in the present polymer-solvent system at 30.0 °C.

Dynamic Light Scattering. Measurements were made for benzene solutions at 30.0 °C on our laboratory-made time interval software correlator of 512 channels. Homodyne time correlation functions $A(t)$ of vertically polarized-scattered-light intensities for the visible PS parts were measured at six different angles from 10 to 150° with a vertically polarized light of a single-frequency 488-nm line emitted from an etalon-equipped 3-W argon-ion laser (Spectra Physics). The details and accuracy of the data acquisition have been described elsewhere.¹ Six sample solutions were prepared in the range of polymer mass concentration $(2.06\text{--}4.88) \times 10^{-3}$ g cm⁻³, which corresponds to $0.844c^* \text{--} 2.00c^*$, with $c^* (\approx [\eta]^{-1} = 2.44 \times 10^{-3}$ g cm⁻³)¹ the overlapping polymer mass concentration, by filtering a given copolymer solution and a solvent into light scattering cells through Millipore filters with pore sizes of 0.5 and 0.2 μm , respectively. These solutions were left for more than 1 week at ca. 30 °C just prior to measurement. The $A(t)$ profiles measured were analyzed through the histogram method, as described in detail in part 1;¹ the normalized scattered-field correlation function for the visible PS part, $g^{(1)}(t)$, was expressed by two or three exponential modes, which were separated distinctly, as

$$g^{(1)}(t) \equiv S_A(q, t)/S_A(q) = \sum_{i=1}^s a_i \exp[-\Gamma_i(q)t] \quad s = 2\text{--}3 \quad (3)$$

Here the characteristic decay rate or the relaxation frequency Γ_i of mode i was given by an average of Γ values over the Γ distribution on the i th histogram. The fractional amplitude a_i for mode i and the Γ distribution $G(\Gamma)$ over all the modes help to express the first cumulant Γ_0 as $\Gamma_0 = \int_0^\infty \Gamma G(\Gamma) d\Gamma = \sum_i a_i \Gamma_i$. In eq 3, $S_A(q, t)$ and $S_A(q)$ are the dynamic and static structure factors, respectively, for the visible PS subchains. With this $g^{(1)}(t)$ function, $A(t)$ is expressed as $A(t) = \beta [g^{(1)}(t)]^2 + 1 + \delta$. β

Table 2. Dynamic Characteristics of the PS-PMMA Diblock Copolymer, BMM313, in Benzene at 30.0 °C^a

	$\theta = 10^\circ$ $qR_G = 0.139$	$\theta = 30^\circ$ $qR_G = 0.412$	$\theta = 60^\circ$ $qR_G = 0.795$	$\theta = 90^\circ$ $qR_G = 1.13$	$\theta = 120^\circ$ $qR_G = 1.38$	$\theta = 150^\circ$ $qR_G = 1.54$	$\theta \rightarrow 0^\circ$ $qR_G = 0$
$c = 2.06 \times 10^{-3} \text{ g cm}^{-3}$							
Γ_{1A}/q^2	1.20	1.21	1.20	1.20	1.22	1.22	1.21 ($D/D_0 = 1.07$) ^b
Γ_3/q^2	4.05	4.41	4.54	5.08	5.22	5.32	4.05 ($\xi_H = 9.73 \text{ nm}$) ^c
Γ_4/q^2	1.43	1.62	1.78	1.90	2.08	2.11	
a_{1A} ^d	0.92	0.89	0.86	0.83 ₆	0.81	0.78	
$c = 2.72 \times 10^{-3} \text{ g cm}^{-3}$							
Γ_{1A}/q^2	0.930	0.932	0.908	0.927	0.923	0.924	0.924 ($D/D_0 = 0.818$)
Γ_3/q^2	3.73	3.72	3.75	3.74	3.73	3.70	3.73 ($\xi_H = 10.5_8 \text{ nm}$)
Γ_4/q^2	1.42	1.59	1.79	1.88	1.96	2.06	
a_{1A}	0.83	0.76	0.70	0.66	0.64	0.60	
$c = 3.09 \times 10^{-3} \text{ g cm}^{-3}$							
Γ_{1A}/q^2	0.777	0.790	0.802	0.797	0.822	0.814	0.800 ($D/D_0 = 0.708$)
Γ_3/q^2	2.90	2.90	2.74	2.65	2.97	2.97	2.85 ($\xi_H = 13.8 \text{ nm}$)
Γ_4/q^2	4.28	3.99	5.00	4.78	10.1 ₃	10.4 ₄	4.51 ($\theta = 10-90^\circ$)
Γ_5/q^2	1.42	1.53	1.73	1.79	1.94	2.08	
a_{1A} ^d	0.80	0.72 ₆	0.64	0.58	0.56	0.55	
a_3 ^d	0.02	0.10	0.23	0.29	0.39	0.41	
$c = 3.47 \times 10^{-3} \text{ g cm}^{-3}$							
Γ_{1A}/q^2	0.746	0.755	0.741	0.754	0.748	0.764	0.751 ($D/D_0 = 0.665$)
Γ_3/q^2	2.51	2.49	2.53	2.48	2.51	2.66	2.50 ($\xi_H = 15.7 \text{ nm}$)
Γ_4/q^2	4.61	3.92	4.77	4.68	10.4 ₈	10.1 ₄	4.49 ($\theta = 10-90^\circ$)
Γ_5/q^2	1.40	1.52	1.73	1.72	2.04	2.16	
a_{1A}	0.77	0.70	0.60	0.56	0.48	0.47	
a_3	0.02	0.11	0.31	0.34	0.45	0.49	
$c = 4.04 \times 10^{-3} \text{ g cm}^{-3}$							
Γ_{1A}/q^2	0.511	0.500	0.499	0.500	0.502	0.500	0.504 ($D/D_0 = 0.446$)
Γ_3/q^2	2.01	2.07	2.05	1.91	2.01	1.93	1.99 ($\xi_H = 19.7 \text{ nm}$)
Γ_4/q^2	4.50	3.91	4.61	4.24	10.8 ₁	10.2 ₈	4.32 ($\theta = 10-90^\circ$)
Γ_5/q^2	1.40	1.51	1.60	1.63	2.12	2.27	
a_{1A}	0.73	0.64	0.52	0.45	0.40	0.39	
a_3	0.07	0.18	0.34	0.40	0.54	0.57	
$c = 4.88 \times 10^{-3} \text{ g cm}^{-3}$							
Γ_{1A}/q^2	0.412	0.396	0.399	0.426	0.406	0.416	0.404 ($D/D_0 = 0.358$)
Γ_3/q^2	1.78	1.82	1.80	1.82	1.87	1.83	1.82 ($\xi_H = 21.6 \text{ nm}$)
Γ_4/q^2	4.85	4.01	4.49	4.34	10.5 ₄	10.5 ₃	4.42 ($\theta = 10-90^\circ$)
Γ_5/q^2	1.30	1.40	1.48	1.53	2.35	2.41	
a_{1A}	0.68	0.57	0.46	0.40	0.35	0.33	
a_3	0.11	0.22	0.42	0.47	0.59	0.63 ₅	

^a Γ_{1A} , Γ_3 , and Γ_4 are mean decay rates of slow mode 1A, medium mode 3, and fast mode 4, respectively, and Γ_1 is the first cumulant. a_i is the fractional amplitude for mode i (Γ_i/q^2 and Γ_1/q^2 are given in units of $10^{-7} \text{ cm}^2 \text{ s}^{-1}$). ^b $D_0 = 1.13 \times 10^{-7} \text{ cm}^2 \text{ s}^{-1}$, the translational diffusion coefficient at infinite dilution estimated in the dilute region.¹ ^c ξ_H is the blob size of the PS part. ^d $a_{1A} + a_3 = 1.0$ for $c = 2.06 \times 10^{-3}$ – $2.72 \times 10^{-3} \text{ g cm}^{-3}$ (the case of two modes), and $a_{1A} + a_3 + a_4 = 1.0$ for $c = 3.09 \times 10^{-3}$ – $4.88 \times 10^{-3} \text{ g cm}^{-3}$ (the case of three modes).

and δ are the factors depending on experimental conditions and represent the spatial coherent condition and the deviation of the $A(t)$ baseline from 1.000, respectively; these values were maintained at $0.4 < \beta < 1$ and $|\delta| \leq 0.003$ in the present experiments.

Results and Discussion

Three Modes of Motion. The time correlation function $A(t)$ measured for the present PS-*block*-PMMA-benzene solutions, which reflects the chain dynamics of the visible PS part, was represented at all q and c by two- or three-mode exponentials whose decay rates Γ_i were separated distinctly from each other. Typical results obtained on the q and c dependences of $\Gamma_i(q, c)$ are presented in Figure 1. Here the decay rates divided by the squared scattered vector, $\Gamma_i(q, c)/q^2$, are demonstrated logarithmically as a function of the concentration c for mode i ($i = 2-3$) at two scattering angles $\theta = 30$ and 120° . The Γ_i/q^2 values at 30 and 120° thus represent typically the chain dynamics at $(qR_G)^2 \ll 1$ and $(qR_G)^2 > 1$, respectively, with R_G the root-mean-square radius of gyration of the diblock chain. The behavior of Γ_i/q^2 in Figure 1 can be divided into two parts by a vertical chain line around $c = 1.9 \times 10^{-3} \text{ g cm}^{-3}$. The right-hand region at $c \geq 2.06 \times 10^{-3} \text{ g cm}^{-3}$ ($=0.844c^*$) is the case we are at present dealing with as the semidilute solutions. Meanwhile the left-hand region at $c \leq 1.60 \times$

$10^{-3} \text{ g cm}^{-3}$ ($=0.657c^*$) is the dilute solution region and has been discussed already in part 1 of this series, where two modes denoted as modes 1 and 2 have been detected. Figure 1 shows that, at four higher different concentrations $c = 3.09, 3.47, 4.04$, and $4.88 \times 10^{-3} \text{ g cm}^{-3}$ ($1.27c^*$ – $2.00c^*$) in the semidilute region, three modes of motion appear. We denote them as mode 1A (slow mode), mode 3 (medium mode), and mode 4 (fast mode) in the order of relaxation speed of motion. At two lower concentrations $c = 2.06$ and $2.72 \times 10^{-3} \text{ g cm}^{-3}$ ($0.844c^*$ and $1.11c^*$) in the semidilute region, on the other hand, only two modes of motion are observed: The slower mode of small Γ/q^2 values can be connected with mode 1 of the dilute solution region, while the faster mode of large Γ/q^2 values seems to be in the position extending from mode 2 of the dilute solution region to mode 3. The former thus includes mode 1A, while the latter is treated at present as mode 3. These two modes cannot completely be treated as the dilute solution behavior in view of their drastic downward departure in the Γ_i/q^2 vs c plots from the linear Γ_i/q^2 - c relation which is characteristic of the dilute solution region. Therefore these two modes at lower c in the semidilute region are regarded as transient modes appearing in a transition region between the dilute solution and higher- c semidilute solution states.

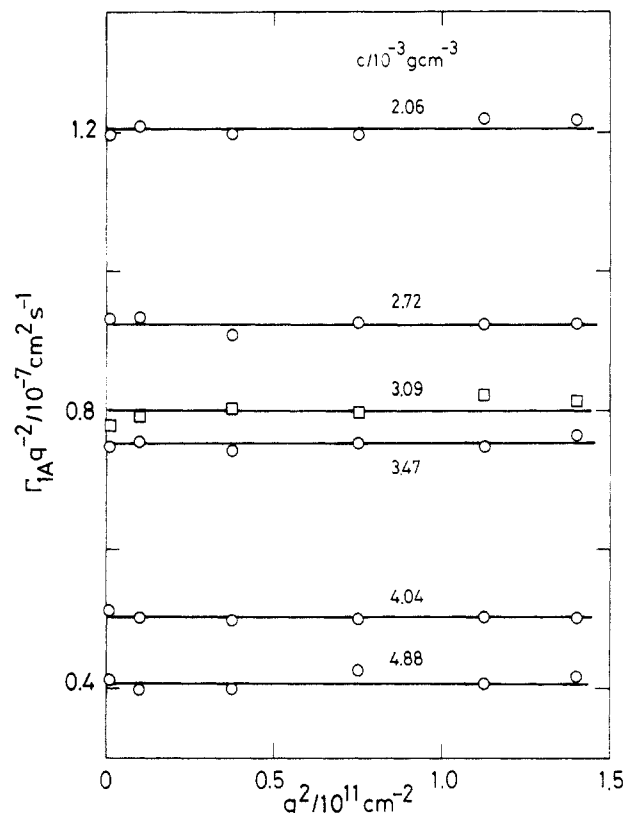


Figure 2. Mean decay rate of the slow mode 1A, $\Gamma_{1A}(q, c)/q^2$, plotted against q^2 for semidilute solutions of the PS-PMMA diblock copolymer in benzene at 30 °C at six concentrations c ranging from 2.06×10^{-3} to $4.88 \times 10^{-3} \text{ g cm}^{-3}$.

The behavior at $\theta = 30$ and 120° expresses the diblock chain dynamics at $(qR_G)^2 \ll 1$ and $(qR_G)^2 > 1$, respectively, as described above. Figure 1 thus indicates that in the semidilute region the slower two modes having Γ_{1A}/q^2 and Γ_3/q^2 values are independent of q and are of strong c dependence, while the fastest mode having Γ_4/q^2 values depends strongly on q but does not depend on c . The detailed results on the q and c dependences of these decay rates Γ_i and the first cumulant Γ_e are summarized in Table 2 and are discussed fully in the following sections.

Slow Mode. Figure 2 shows plots of $\Gamma(q, c)/q^2$ vs q^2 at six different concentrations c obtained for the slowest mode 1A of the semidilute solutions of PS-PMMA in benzene. The c values are given by 2.06 – 4.88 ($\times 10^{-3} \text{ g cm}^{-3}$) indicated beside the data points. As is clearly shown in the figure, the $\Gamma_{1A}(q, c)/q^2$ values are constant over all q at a fixed c , that is, Γ_{1A} is proportional to q^2 at a given c in the range $0.13 < qR_G < 1.54$. This means that mode 1A represents a diffusion motion and that the average value of $\Gamma_{1A}(q, c)/q^2$ over six different q gives the value at $q \rightarrow 0$, i.e., a long-time diffusion coefficient at finite c ; $D_{1A}(c) = [\Gamma_{1A}(q, c)/q^2]_{q \rightarrow 0}$. It should also be noted, as shown in Figure 1, that this $D_{1A}(c)$ value follows the $[\Gamma_1(q, c)/q^2]_{q \rightarrow 0}$ values which have been observed for mode 1 in the dilute region and then decreases exponentially with increasing c . Here $[\Gamma_1(q, c)/q^2]_{q \rightarrow 0}$ has been identified as $D_{\text{copol}}(c)$, which represents the center-of-mass diffusion coefficient of the entire copolymer chain, i.e., the long-time translational diffusion coefficient of the PS-PMMA chain;¹ for the long times the diffusion of the PS part feels the effect of the invisible PMMA part, and the PS and PMMA parts diffuse together. A permanent network is considered to be formed around a critical concentration $c = 3.5c^* - 4c^*$, as will be described in a later section. Since the critical value is beyond the present region of $c = 0.844c^* - 2.00c^*$, the observed mode 1A represents the center-of-mass diffusion

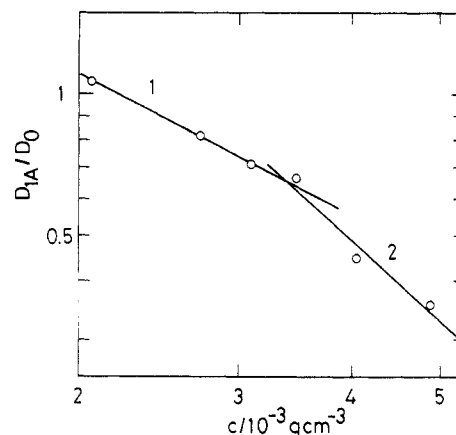


Figure 3. Ratio of the diffusion coefficient of the slow mode $D_{1A}(c)$ in the semidilute region to the translational diffusion coefficient D_0 in the dilute region, $D_{1A}(c)/D_0$, plotted logarithmically against c . The slopes of lines 1 and 2 are -1 and -1.75 , respectively.

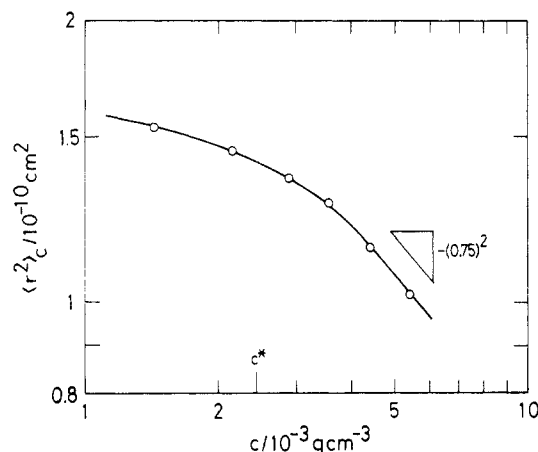


Figure 4. Mean-square distance between the centers of mass of two different PS subchains, $\langle r^2 \rangle_c$, plotted logarithmically against c for semidilute solutions of the PS-PMMA diblock copolymer in benzene at 30 °C. c^* denotes the overlapping polymer mass concentration, $c^* = 2.44 \times 10^{-3} \text{ g cm}^{-3}$. The asymptotic slope at higher c is roughly $-(0.75)^2$.

of a single PS-PMMA block chain in a pregel state, rather than the reptation motion occurring in the polymer chain network.

The ratio of $D_{1A}(c)$ to the dilute limit, $D_{1A}(c)/D_0$, is plotted logarithmically against c in Figure 3, with D_0 ($\equiv D_{1A}(c=0) = 1.13 \times 10^{-7} \text{ cm}^2 \text{ s}^{-1}$) the long-time translational diffusion coefficient of the block chain (mode 1) at infinite dilution.¹ The exponent δ in the expression $D_{1A}(c)/D_0 \sim c^\delta$ changes from ca. -1.0 to ca. -1.75 with increasing c . Although the PS-PMMA block chain is in a pregel state, the exponent δ obtained above is equal roughly to -1.75 , which is expected for the self-diffusion of the chain (reptation). This characteristic concentration dependence will be due to strong interactions of the PS-PMMA block chain with its surrounding matrix chains. As shown in Figure 4, the mean-square distance between the centers of mass of the two different PS subchains, $\langle r^2 \rangle_c$, decreases with increasing c in the concentration region in question¹¹ and gives a rough limiting relation $\langle r^2 \rangle_c \sim c^{-(0.75)^2}$ at $c > 4 \times 10^{-3} \text{ g cm}^{-3}$. The logarithmic plot of $D_{1A}(c)$ vs $\langle r^2 \rangle_c$ shows finally a positive linear relation expressed by the solid line in Figure 5, which represents a relation $D_{1A}(c) = 2.65 \times 10^{30} \langle r^2 \rangle_c^{3.80} (\text{cm}^2 \text{ s}^{-1})$ over all c measured. This result means that the diffusion speed of the block chain decreases exponentially with decreasing mean-square distance between the centers of mass of two PS subchains.

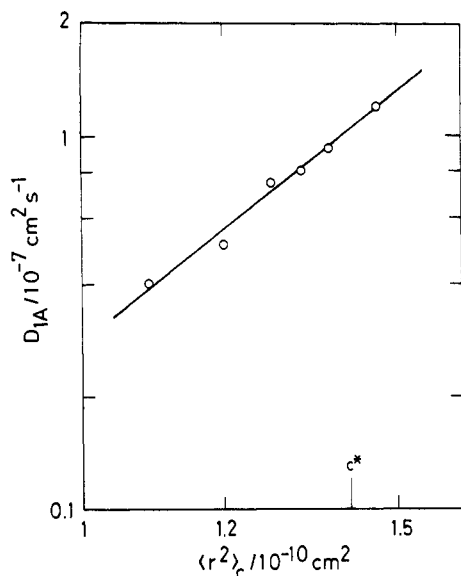


Figure 5. Logarithmic plot of $D_{1A}(c)$ vs $\langle r^2 \rangle_c$ for semidilute solutions of the PS-PMMA diblock copolymer in benzene at 30 °C. The slope of the data-fitted line is 3.80.

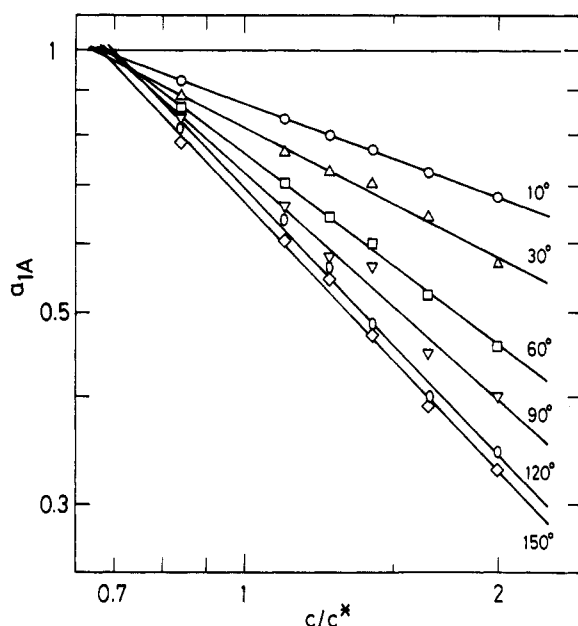


Figure 6. Concentration dependence of the fractional amplitude of the slow mode, $a_{1A}(q,c)$, plotted in the logarithmic scales for semidilute solutions of the PS-PMMA diblock copolymer in benzene at 30 °C at six scattering angles ranging from 10 to 150°.

Figure 6 shows the concentration dependence of the fractional amplitude for mode 1A, $a_{1A}(q,c)$ at a given q in the logarithmic plots of a_{1A} vs c/c^* . a_{1A} for each q decreases with increasing c and shows linear dependences on c in the logarithmic scales. The slopes (negative values) increase with increasing q as -0.36 ($\theta = 10^\circ$) to -1.0 ($\theta = 150^\circ$), and all the data points seem to converge into a common point at $a_{1A} = 1$ with $[c/c^*]_{a_{1A}=1} \approx 0.68$. This feature is in clear conflict with the a_1 behavior in the dilute solution region where the $a_1(c)$ vs c plots have shown linear relations and the slopes have changed from negative to positive with increasing q .

Medium Mode. In Figure 7, the decay rates of the medium mode (mode 3), $\Gamma_3(q,c)/q^2$, are plotted against both q^2 and $(qR_G)^2$ at six concentrations c .¹² Except for a case on the lowest c of $c = 2.06 \times 10^{-3} \text{ g cm}^{-3}$, which is in a transition region as mentioned already, the Γ_3/q^2 values at fixed c are constant, irrespective of q , that is, Γ_3/q^2 is independent of q over the range $0.019 \leq (qR_G)^2 \leq 2.36$.

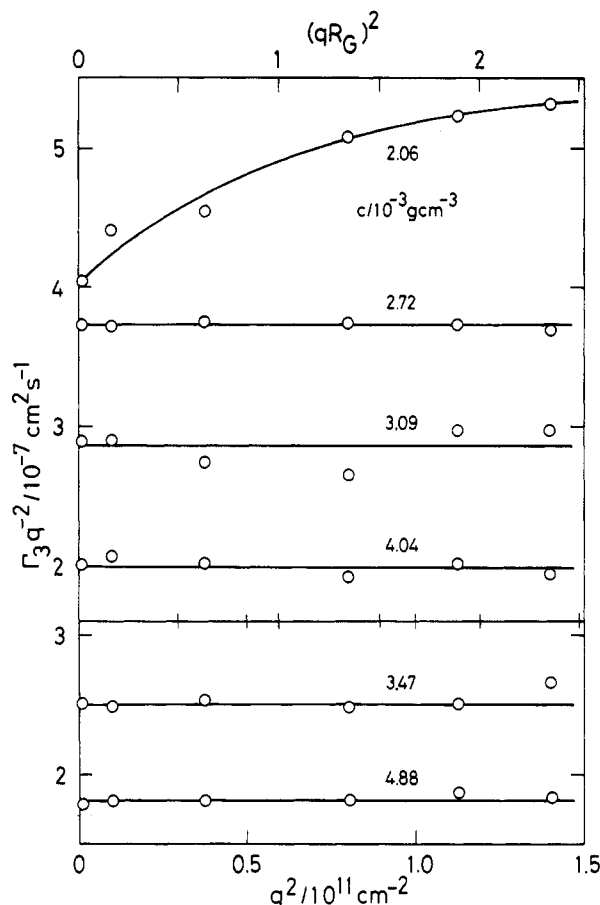


Figure 7. Mean decay rate of the medium mode 3, $\Gamma_3(q,c)/q^2$, plotted against q^2 and $(qR_G)^2$ for semidilute solutions of the PS-PMMA diblock copolymer in benzene at 30 °C at six concentrations c ranging from 2.06×10^{-3} to $4.88 \times 10^{-3} \text{ g cm}^{-3}$.

Averaging these values for each c , we estimated the limiting $q \rightarrow 0$ value at a given c , i.e., $[\Gamma_3(c)/q^2]_{q \rightarrow 0}$. The present medium mode 3, therefore, represents a diffusion motion, but the value (the diffusion coefficient) thus obtained is about 4 times larger than that of the slow mode $D_{1A}(c) = [\Gamma_{1A}(c)/q^2]_{q \rightarrow 0}$ for each c .

The fractional amplitude of mode 3, $a_3(q,c)$, increases exponentially with increasing c , as shown in Figure 8 in the logarithmic plots of a_3 vs c/c^* . For each scattering angle, four data points at higher c could be extrapolated linearly to unity ($a_3 = 1$) and the critical c at $a_3 = 1$ could be estimated as $c = 3.5c^* - 4c^*$, irrespective of q . This a_3 behavior means that a permanent network is formed above $c \approx 3.5c^* - 4c^*$ and the region observed in this paper ($c \leq 2.0c^*$) is still in a pregel state. These results on the q independence of $\Gamma_3(c)/q^2$ and on the a_3 behavior allow us to assign this motion to be a cooperative diffusion of the PS (concentration) blob, the inner conformation of the PS blobs being shielded from the neighboring PS and PMMA chains, and the PS blobs moving freely in the solution.

The cooperative diffusion coefficient at finite c , i.e., $D_{\text{coop,PS}}(c)$ defined now by $D_{\text{coop,PS}}(c) = [\Gamma_3(c)/q^2]_{q \rightarrow 0}$, gives a relation $D_{\text{coop,PS}} \propto c^{-1}$ at higher c , as indicated in Figure 9. However, as described below, this c dependence disagrees with the scaling prediction for the cooperative diffusion at $\xi_H \ll q^{-1} \ll R_G$ (the so-called "pseudogel" state) in semidilute solutions.¹³ Here ξ_H denotes a screening length or the radius of PS concentration blobs and can be estimated by using a relation¹⁴

$$\xi_H(c) = k_B T (1 - \phi_P)^2 / 6 \pi \eta_s D_{\text{coop,PS}}(c) \quad (4)$$

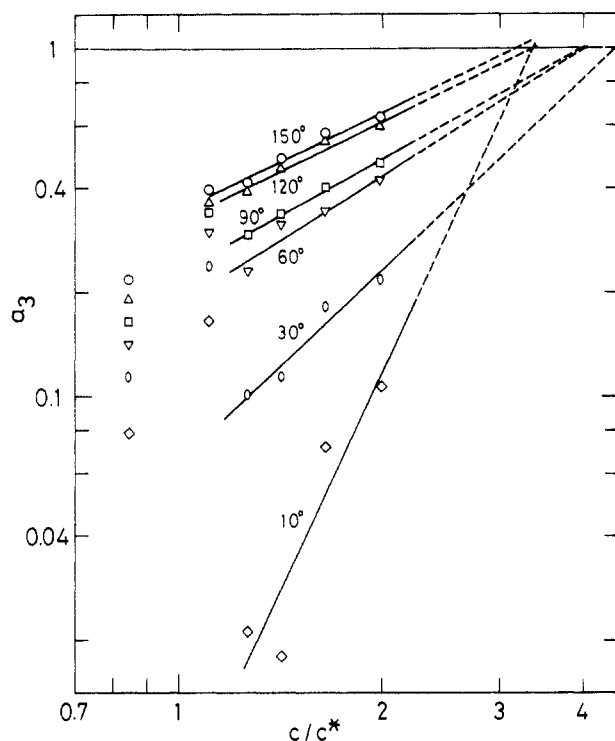


Figure 8. Fractional amplitude of the medium mode $a_3(q, c)$ plotted against c/c^* for semidilute solutions of the PS-PMMA diblock copolymer in benzene at 30 °C at six scattering angles of 10–150°. For each scattering angle, four data points at higher c can be extrapolated linearly to $a_3(q, c) = 1$.

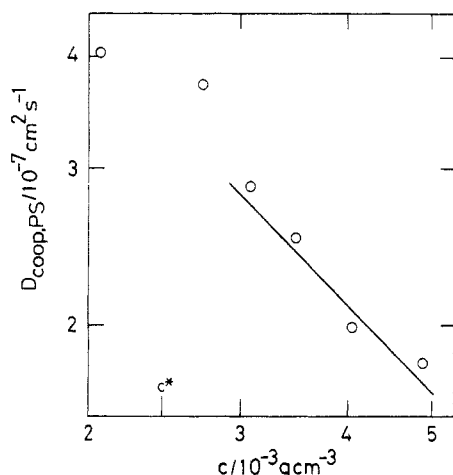


Figure 9. The concentration dependence of the cooperative diffusion coefficient $D_{\text{coop,PS}}(c)$ estimated from the medium mode for semidilute solutions of the PS-PMMA diblock copolymer in benzene at 30 °C. The logarithmic plot gives roughly a slope -1 in the high- c region.

with ϕ_P the volume fraction of the block copolymer.¹⁵ Over all c and q measured, $q\xi_H$ was found to range from 0.033 to 0.81 (i.e., $q^{-1} > \xi_H$), while qR_G ranged from 0.13 to 1.54. In view of the scaling concepts of the hydrodynamic screening and the concentration (Rouse) blobs of radius ξ_H , it is possible to predict the dynamical aspects of the present PS-PMMA diblock chains (the PMMA part is invisible optically) in semidilute solution in the following way. Let the position \mathbf{r}_j of the j segment in a PS subchain P be expressed as $\mathbf{r}_j = \mathbf{r}_P + \mathbf{r}_{PA} + \mathbf{r}_{AK} + \mathbf{r}_{Kj}$ with \mathbf{r}_P the center-of-mass position of the block chain, \mathbf{r}_{PA} the distance between the centers of mass of the block chain and the PS subchain, \mathbf{r}_{AK} the distance between the centers of mass of the PS subchain and a blob K within the subchain, and \mathbf{r}_{Kj} the distance of the j segment (within blob K) from the center of mass of the blob K.

We assume that \mathbf{r}_P of different chains and $\mathbf{r}_P, \mathbf{r}_{PA}, \mathbf{r}_{AK}$, and \mathbf{r}_{jk} of the same chain are uncorrelated with each other and assume that the interactions between the PS and PMMA subchains are neglected. Since motions between different blobs are uncorrelated due to the hydrodynamic screening, $S(q, t)$ can be broken down into contributions due to chain P, PS-PMMA subchains, PS-blob K within chains, and segments j and k within blobs. $S(q, t)$ then gives features characteristic of the experimental scale of measure q^{-1} : (1) At $q^{-1} \ll \xi_H$, $S(q, t)$ becomes

$$S(q, t) \propto \langle \exp[i\mathbf{q} \cdot (\mathbf{r}_{Kj}(0) - \mathbf{r}_{Kk}(t))] \rangle \quad (5)$$

and the segmental motions within blobs are predicted, which resemble basically single-chain dynamics. (2) In the pseudogel region where $\xi_H \ll q^{-1} \ll R_G$, we have

$$S(q, t) \propto \langle \exp[i\mathbf{q} \cdot (\mathbf{r}_{PA}(0) - \mathbf{r}_{PA}(t))] \exp[i\mathbf{q} \cdot (\mathbf{r}_{AK}(0) - \mathbf{r}_{AK}(t))] \rangle \quad (6)$$

From the first part of (...), which represents the distance fluctuation between the centers of mass of the PS and PMMA subchains, the internal mode of motion is predicted. Rouse dynamics will be effective in understanding the behavior in this case. The second part of (...), on the other hand, represents the motion of the center of mass, or the cooperative diffusion process, of a concentration blob of radius ξ_H . The diffusion coefficient D_{coop} is then expected to be $D_{\text{coop}} \propto c^{0.75}$ in a good solvent limit or $D_{\text{coop}} \propto c^{0.5}$ in a transition region. (3) At $q^{-1} \gtrsim R_G$, it becomes

$$S(q, t) \propto \langle \exp[i\mathbf{q} \cdot (\mathbf{r}_P(0) - \mathbf{r}_P(t))] \rangle \quad (7)$$

At $t \rightarrow \infty$, $S(q, t)$ predicts the center-of-mass diffusion of the entire copolymer chain or the long-time diffusion coefficient D_{copol} with $D_{\text{copol}} \propto c^{-1.75}$. At the short-time limit, $S(q, t)$ predicts the diffusion of PS subchains, which reflects the first cumulant Γ_e .

As described already, experimental $D_{\text{coop,PS}}(c)$ values, defined by $[\Gamma_3(c)/q^2]_{q \rightarrow 0}$, are found to show the c^{-1} dependence in both regions of $\xi_H \ll q^{-1} \ll R_G$ (case 2) and $q^{-1} \gtrsim R_G$ (case 3). This result disagrees with the scaling predictions that $D_{\text{coop}} \propto c^{0.75}$ or $D_{\text{coop}} \propto c^{0.5}$. Coupling between the cooperative diffusion and internal motions^{9,10} could be expected except for the two cases in the short-time and Markoff limits.

Fast Mode. The third mode (mode 4) was detected only for four solutions of concentration higher than $c = 3.09 \times 10^{-3} \text{ g cm}^{-3}$. Its decay rates are the largest of the observed three modes and the values, $\Gamma_4(q, c)/q^2$, are about 2–5 times larger than those of the medium mode (mode 3) at each q , as listed in Table 2. In Figure 10, $\Gamma_4(q, c)/q^2$ is plotted against c for four higher c at fixed q . These plots indicate that, over c measured, Γ_4/q^2 at given q is roughly constant to c to within experimental errors of $\pm 5\%$ or less, as the average value is shown by a horizontal line at each q . This c independence conflicts with the rough c^{-1} dependence observed already for mode 3 over all q . The q dependence of $\Gamma_4(q, c)$ at four c values is then given in Figure 11 in the logarithmic plots of Γ_4 vs q^2 . As is clear in the figure, Γ_4 values at four c are roughly independent of c , and their q dependences give a relation $\Gamma_4 \propto q^2$ at smaller q , or more strictly $\Gamma_4 = 4.44 \times 10^{-7} q^2 \text{ (s}^{-1}\text{)}$ at $(qR_G)^2 < 1.2$, while at larger q they indicate a different relation $\Gamma_4 \propto q^{4.5}$ at $(qR_G)^2 > 1.3$.¹² This behavior suggests that mode 4 is deeply related to the internal motions.

According to a very recent renormalization group calculations,¹⁶ the internal mode of motion of both Gaussian and self-avoiding chains is predicted to exhibit

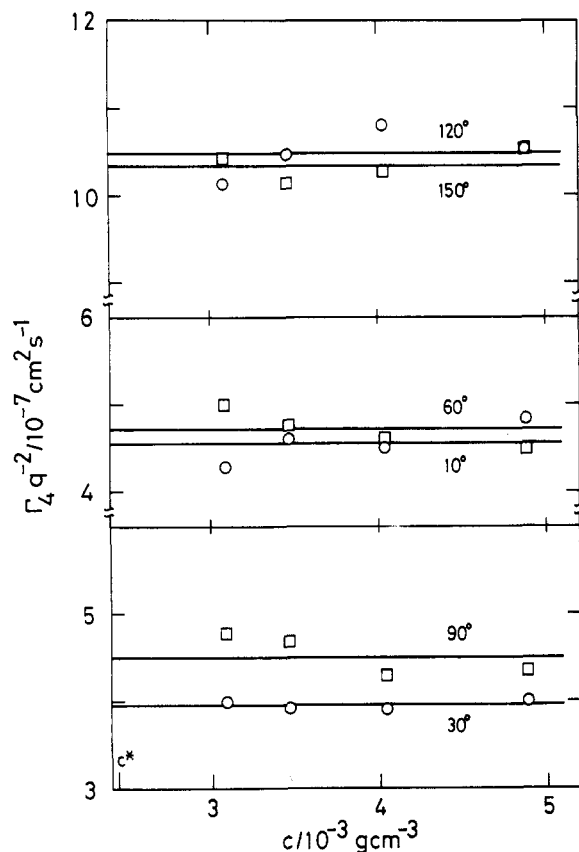


Figure 10. Mean decay rate of the fast mode 4, $\Gamma_4(q,c)/q^2$, plotted against c for semidilute solutions of the PS-PMMA diblock copolymer in benzene at 30 °C at six scattering angles of $\theta = 10$ – 150° : (O) 10° , 30° , 120° ; (□) 60° , 90° , 150° . For each θ , four data points are shown since the fast mode was observed only for four high- c solutions.

Rouse-like behavior in semidilute solutions since in this case the hydrodynamic and excluded volume interactions become totally screened out, and the behavior is in accord with the scaling predictions. Internal motion based on Rouse dynamics has been given for diblock copolymer chains^{10,6} with the predictions that the decay rate of internal motion Γ_{int} decreases with decreasing q at $qR_G \ll 1$ and takes a nonzero constant value $\Gamma_{\text{int}}(q=0)$ at $q \rightarrow 0$, though the fractional amplitude a_{int} vanishes as $q \rightarrow 0$, while Γ_{int} shows q^4 dependence at $qR_G \gg 1$.

The q^{4-5} dependence of experimental $\Gamma_4(q,t)$ at $(qR_G)^2 > 1.3$ agrees roughly with the above-mentioned prediction from Rouse dynamics. This indicates that the internal motion of diblock copolymers in a good solvent does not suffer any hydrodynamic nor excluded volume interactions. The experimental relation $\Gamma_4(c) = 4.44 \times 10^{-7} q^2$ obtained at $(qR_G)^2 < 1.2$, on the other hand, is in conflict with the prediction from Rouse dynamics where Γ_4 is to approach a q -independent constant as $q \rightarrow 0$. The diffusion coefficient like value, $4.44 \times 10^{-7} \text{ cm}^2 \text{ s}^{-1}$, which is roughly independent of c , is about twice as large as $D_{\text{coop,PS}}(c)$ of mode 3. The Γ_4 motion is about twice as fast as the cooperative diffusion of the PS blobs. In addition, the fractional amplitude of mode 4, $a_4(q,c)$ is found to increase slightly with decreasing $(qR_G)^2$, as is shown in Figure 12, and reaches a nonzero value, $(a_4)_{q \rightarrow 0} \simeq 0.2$, as $(qR_G)^2 \rightarrow 0$. This a_4 behavior disagrees again with the prediction for internal motion that $a_{\text{int}} \rightarrow 0$ as $q \rightarrow 0$. Even if Rouse dynamics holds in semidilute solution, the cooperative diffusion and interdiffusion couple with each other.^{9,10} Mode 4 thus cannot be identified simply with the interdiffusion process, and neither directly attributes the constant term, $\Gamma_4(c)/q^2$ at $(qR_G)^2 < 1.2$, to the relative

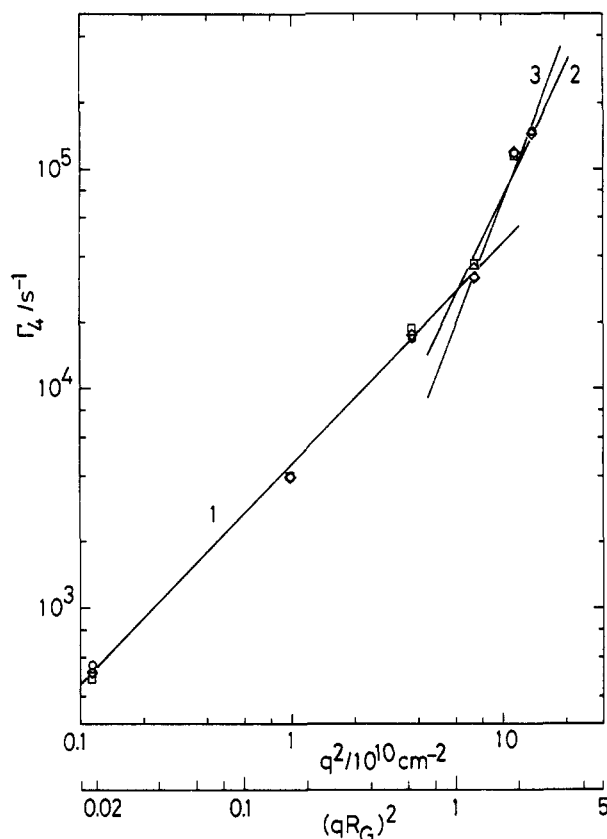


Figure 11. Logarithmic plots of the mean decay rate of the fast mode $\Gamma_4(q,c)$ against both q^2 and $(qR_G)^2$ for semidilute solutions of the PS-PMMA diblock copolymer in benzene at 30 °C: (□) $c = 3.09 \times 10^{-3} \text{ g cm}^{-3}$; (Δ) $c = 3.47 \times 10^{-3} \text{ g cm}^{-3}$; (◇) $c = 4.04 \times 10^{-3} \text{ g cm}^{-3}$; (○) $c = 4.88 \times 10^{-3} \text{ g cm}^{-3}$. Lines 1–3 are straight lines with slopes 1 ($\Gamma_4 \propto q^2$), 2 ($\Gamma_4 \propto q^4$), and 2.5 ($\Gamma_4 \propto q^5$), respectively.

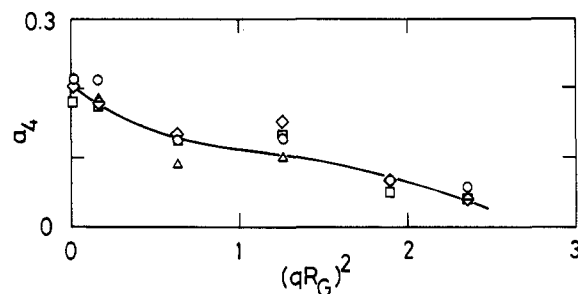


Figure 12. Fractional amplitude of the fast mode, $a_4(q,c)$, plotted against $(qR_G)^2$ for four semidilute solutions of the PS-PMMA diblock copolymer in benzene at 30 °C. Symbols are the same as in Figure 11.

motion of the collective PS subchains with respect to the collective PMMA subchains. PS and PMMA blobs may not correlate in their semidilute solutions due to the hydrodynamic screening (Rouse-like behavior), but the relaxation of thermal fluctuations in the relative local concentrations of a pair of PS and PMMA subchains toward their equilibrium value still happens in these semidilute solutions. The constant Γ_4/q^2 term will originate in such fluctuations.

First Cumulant. Figure 13 shows the concentration dependence of the first cumulant $\Gamma_1(q,c)/q^2$ at fixed q . When c is less or around c^* , the Γ_1/q^2 values at each q indicate no clear c dependence but connect smoothly with the dilute solution values at the corresponding q , which have been shown in Figure 11 of part 1.¹ At $c \geq c^*$, however, Γ_1/q^2 shows a distinct linear relation to c for each q . The slope changes from negative to positive with increasing q , the c dependence being completely inverse in the case of

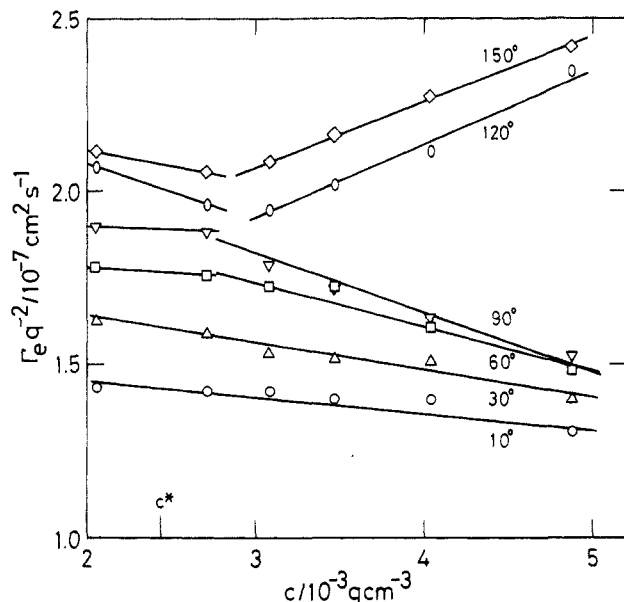


Figure 13. Concentration dependence of the first cumulant $\Gamma_e(q,c)/q^2$ for semidilute solutions of the PS-PMMA diblock copolymer in benzene at 30 °C at six scattering angles of 10–150°.

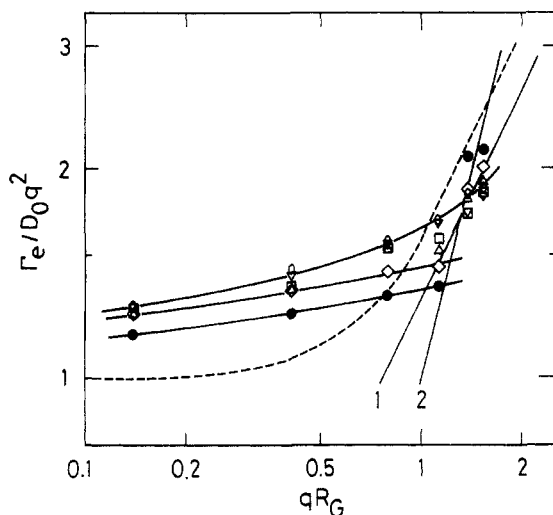


Figure 14. Re-formed first cumulant $\Gamma_e(q,c)/D_0q^2$ plotted against qR_G in the logarithmic scales for semidilute solutions of the PS-PMMA diblock copolymer in benzene at 30 °C: (○) $c = 2.06 \times 10^{-3} \text{ g cm}^{-3}$; (▽) $c = 2.72 \times 10^{-3} \text{ g cm}^{-3}$; (□) $c = 3.09 \times 10^{-3} \text{ g cm}^{-3}$; (Δ) $c = 3.47 \times 10^{-3} \text{ g cm}^{-3}$; (◇) $c = 4.04 \times 10^{-3} \text{ g cm}^{-3}$; (●) $c = 4.88 \times 10^{-3} \text{ g cm}^{-3}$. At $qR_G > 1$ the data for $c = 4.88 \times 10^{-3} \text{ g cm}^{-3}$ approach line 2 with a slope of 2, i.e., $\Gamma_e \propto q^4$. The broken curve represents the experimental first cumulant obtained in the dilute region,¹ $(\Gamma_e)_{c \rightarrow 0}/D_0q^2$, the slope approaching 1 at $qR_G > 1$.

the dilute solution region (part 1). These features can be demonstrated more clearly in Figure 14. Here the $\Gamma_e(q,c)/D_0q^2$ values at six different c of $(2.06\text{--}4.88) \times 10^{-3} \text{ g cm}^{-3}$ are plotted logarithmically against qR_G with D_0 and R_G the translational diffusion coefficient and the radius of gyration at infinite dilution, respectively; $D_0 = 1.13 \times 10^{-7} \text{ cm}^2 \text{ s}^{-1}$ and $R_G = 41.0 \text{ nm}$.¹ Firstly, it is found that the data points are located far above unity even at $qR_G \ll 1$. Since the motion in this region represents the short-time diffusion motion,¹⁰ the short-time values, $\Gamma_e(q,c)/q^2$, are to correspond to the values for homo-PS of the same molecular weight as the PS subchain and are to compare with the long-time ones, D_{copoly} , which were estimated from the slow mode 1A as the q -independent values, $[D_{1A}(c)/q^2]_{q \rightarrow 0}$. Though no difference is predicted theoretically between the short- and long-time behaviors in Rouse dynamics, the short-time values are found to be larger

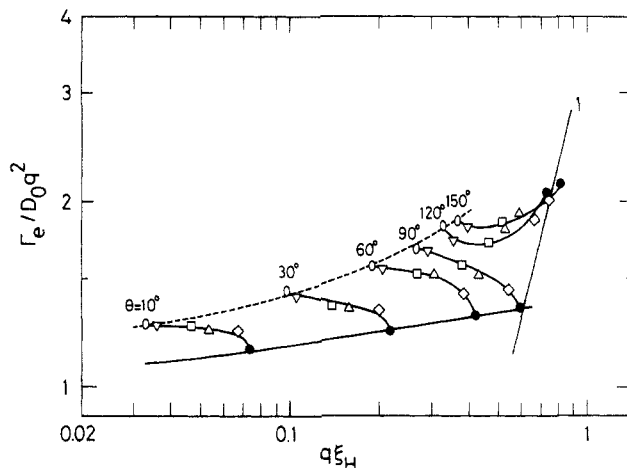


Figure 15. Replots of the first cumulant in Figure 14 against $q\xi_H$ in the logarithmic scales. ξ_H denotes the blob size of the PS part. Symbols are the same as in Figure 14. The broken curve is an eye guide for data at $c = 2.06 \times 10^{-3} \text{ g cm}^{-3}$. Line 1 is a straight line with a slope of 2.0 ($\Gamma_e \propto q^4$).

than the long-time ones in all c , as shown in Table 2, and the equality between them cannot be expected. Secondly, the Γ_e/D_0q^2 vs qR_G behavior changes with c . As shown in Figure 14, Γ_e/q^2 for solutions of $c \leq c^*$ increases gradually with qR_G over the range $qR_G = 0.13\text{--}1.54$. For solutions of higher c , however, a transition of Γ_e to $q^3 \sim q^4$ occurs at $qR_G \approx 1.1$. In other words, the slope at $qR_G > 1.1$ becomes steeper for higher c ; e.g., $\Gamma_e \propto q^3$ (line 1 with a slope of 1) for solutions of $c = 4.04 \times 10^{-3} \text{ g cm}^{-3}$ (diamonds) and $\Gamma_e \propto q^4$ (line 2 with a slope of 2) for solutions of $c = 4.88 \times 10^{-3} \text{ g cm}^{-3}$ (filled circles). This indicates that the internal motions in the semidilute solution approach in the high-concentration region the draining q^4 dependency, or Rouse dynamics. This result is different from the internal motions observed in the dilute solution limit¹ where the limiting value $(\Gamma_e)_{c \rightarrow 0}/D_0q^2$ is, as demonstrated in the same figure by a broken line, constant (unity) at small qR_G and changes at $qR_G \approx 1$ to the nondraining q^3 dependency (slope 1).

According to the blob hypothesis, the above-mentioned transition will occur at $q\xi_H = 1$, not at $qR_G = 1$. With the ξ_H values estimated in the Medium Mode section, the Γ_e/D_0q^2 values in Figure 14 are replotted logarithmically against $q\xi_H$ in Figure 15. The data points are located in the region $0.033 < q\xi_H < 0.81$. Typically shown by the data for the lowest c of $c = 2.06 \times 10^{-3} \text{ g cm}^{-3}$ (open circles) and demonstrated by a broken curve, Γ_e/q^2 at lower fixed c values increases slowly with increasing $q\xi_H$ and indicates that the data are in a broad transition region within the $q\xi_H$ measured. At fixed q , however, these data are grouped into branched lines characteristic of each q and each branch seems to converge to a point of the highest c (filled circles for $c = 4.88 \times 10^{-3} \text{ g cm}^{-3}$) with increasing c . The filled circles then show a clear transition at $q\xi_H \approx 0.6$. The slope of the Γ_e/D_0q^2 vs $q\xi_H$ plot changes from 0.07 (roughly) to 2.0, and the Γ_e transition to q^4 occurs at $q\xi_H \approx 0.6$.

In conclusion, the dynamic structure factor for the well-swollen PS-PMMA diblock copolymer chain in a semidilute solution was found to be expressed by the sum of two exponentials in its lower c regions or of three exponentials in the higher c regions, if one component, i.e. the PMMA part, of the block chain was made invisible optically. These two or three modes of motion were discussed in detail with the existing theoretical models which have predicted two normal modes of motion, although the two modes cannot in general be identified with the cooperative and interdiffusion motions due to

the coupling between them. The theoretically proposed coupling between the cooperative and interdiffusion motions was demonstrated experimentally. However, beyond the theoretical predictions, several new aspects on the diblock chain dynamics were detected through the present experiments, as was made evident specifically by the existence of three modes of motions. These results will be helpful in improving the theoretical considerations or in developing new ones on the dynamics of diblock copolymer chains in solution.

References and Notes

- (1) Tsunashima, Y.; Kawamata, Y. *Macromolecules* **1993**, *26*, 4899.
- (2) Borsali, R.; Fisher, E. W.; Benmouna, M. *Phys. Rev. A* **1991**, *43*, 5732.
- (3) Duval, M.; Haida, H.; Lingelser, J. P.; Gallot, Y. *Macromolecules* **1991**, *24*, 6867.
- (4) Koňák, Č.; Podešva, J. *Macromolecules* **1992**, *24*, 6502.
- (5) Balsara, N. P.; Stepanek, P.; Lodge, T. P.; Tirrell, M. *Macromolecules* **1991**, *24*, 6227.
- (6) Benmouna, M.; Benoit, H.; Borsali, R.; Duval, M. *Macromolecules* **1987**, *20*, 2620.
- (7) Benmouna, M.; Benoit, H.; Duval, M.; Akcasu, A. Z. *Macromolecules* **1987**, *20*, 1107.
- (8) Akcasu, A. Z.; Hammouda, B.; Lodge, T. P.; Han, C. C. *Macromolecules* **1984**, *17*, 759.
- (9) Akcasu, A. Z.; Nägele, G.; Klein, R. *Macromolecules* **1991**, *24*, 4408.
- (10) Akcasu, A. Z. *Dynamic Light Scattering. The method and Some Applications*; Brown, W., Ed.; Clarendon: Oxford, U.K., 1993; Chapter 1.
- (11) Utiyama, H.; Takenaka, K.; Mizumori, M.; Fukuda, M. *Macromolecules* **1974**, *7*, 28.
- (12) $R_G = 41.0$ nm, the root-mean-square radius of gyration at infinite dilution obtained in the dilute region (Part 1 in this series¹).
- (13) Schaefer, D. W.; Han, C. C. In *Dynamic Light Scattering*; Pecora, R., Ed.; Plenum: New York, 1985; Chapter 5.
- (14) Vink, H. *J. Chem. Soc., Faraday Trans. 1* **1985**, *81*, 1725. See also pp 276 and 474 of the book cited in ref 10.
- (15) ϕ_P is related to the polymer mass concentration c [g cm^{-3}] as $\phi_P = \nu c$ with ν the specific volume of the PS-PMMA diblock copolymer; $\nu = (M_{PS}\nu_{PS} + M_{PMMA}\nu_{PMMA})/M$ with $\nu_{PS} = 0.917$ and $\nu_{PMMA} = 0.818 \text{ cm}^3 \text{ g}^{-1}$ in benzene.
- (16) Shiwa, Y. *J. Phys. II* **1993**, *3*, 477.